Ecological Applications, 10(2), 2000, pp. 449–469
© 2000 by the Ecological Society of America

DYNAMIC SIMULATION OF TREE–GRASS INTERACTIONS FOR GLOBAL CHANGE STUDIES

CHRISTOPHER DALY,[1] DOMINIQUE BACHELET,[1] JAMES M. LENIHAN,[1] RONALD P. NEILSON,[2] WILLIAM PARTON,[3] AND DENNIS OJIMA[3]

[1]*Oregon State University, Corvallis, Oregon 97331-2204 USA*
[2]*USDA Forest Service, Corvallis, Oregon 97331 USA*
[3]*Colorado State University, Fort Collins, Colorado 80523 USA*

Abstract. The objective of this study was to simulate dynamically the response of a complex landscape, containing forests, savannas, and grasslands, to potential climate change. Thus, it was essential to simulate accurately the competition for light and water between trees and grasses. Accurate representation of water competition requires simulating the appropriate vertical root distribution and soil water content. The importance of different rooting depths in structuring savannas has long been debated. In simulating this complex landscape, we examined alternative hypotheses of tree and grass vertical root distribution and the importance of fire as a disturbance, as they influence savanna dynamics under historical and changing climates. MC1, a new dynamic vegetation model, was used to estimate the distribution of vegetation and associated carbon and nutrient fluxes for Wind Cave National Park, South Dakota, USA. MC1 consists of three linked modules simulating biogeography, biogeochemistry, and fire disturbance. This new tool allows us to document how changes in rooting patterns may affect production, fire frequency, and whether or not current vegetation types and life-form mixtures can be sustained at the same location or would be replaced by others. Because climate change may intensify resource deficiencies, it will probably affect allocation of resources to roots and their distribution through the soil profile. We manipulated the rooting depth of two life-forms, trees and grasses, that are competing for water. We then assessed the importance of variable rooting depth on ecosystem processes and vegetation distribution by running MC1 for historical climate (1895–1994) and a GCM-simulated future scenario (1995–2094). Deeply rooted trees caused higher tree productivity, lower grass productivity, and longer fire return intervals. When trees were shallowly rooted, grass productivity exceeded that of trees even if total grass biomass was only one-third to one-fourth that of trees. Deeply rooted grasses developed extensive root systems that increased N uptake and the input of litter into soil organic matter pools. Shallowly rooted grasses produced smaller soil carbon pools. Under the climate change scenario, NPP and live biomass increased for grasses and decreased for trees, and total soil organic matter decreased. Changes in the size of biogeochemical pools produced by the climate change scenario were overwhelmed by the range of responses across the four rooting configurations. Deeply rooted grasses grew larger than shallowly rooted ones, and deeply rooted trees outcompeted grasses for resources. In both historical and future scenarios, fire was required for the coexistence of trees and grasses when deep soil water was available to trees. Consistent changes in fire frequency and intensity were simulated during the climate change scenario: more fires occurred because higher temperatures resulted in decreased fuel moisture. Fire also increased in the deeply rooted grass configurations because grass biomass, which serves as a fine fuel source, was relatively high.

Key words: belowground processes and global change; belowground resources; climate change; dynamic vegetation model; fire; global change; grassland; MC1; root distribution; savanna; tree–grass competition; water availability; Wind Cave National Park, South Dakota.

INTRODUCTION

Savannas, woodlands, shrublands, grasslands, and arid lands occupy between 45% and 52% of the world's vegetated land surface (Lieth 1975, Matthews 1983). To varying degrees, both competition for resources between woody and grass vegetation and disturbance by grazing and by fire are thought to control much of the vegetation structure in these complex landscapes. The role of vertical root distributions in structuring these complex ecosystems has long been debated. Roots of both woody and herbaceous plants are generally con-

Manuscript received 18 September 1998; revised 19 February 1999; accepted 23 February 1999; final version received 19 March 1999. For reprints of this Invited Feature, see footnote 1, p. 397.

centrated in surface soil layers (Davis et al. 1983, Jonsson et al. 1988, Dhyani et al. 1990, Nambiar 1990). However, to explain the coexistence of grasses and trees in dry savannas, Walter (1971) hypothesized that grass roots occupied shallow soil layers and appropriated rainfall infiltrating the soil surface, whereas tree roots were located deeper in the profile and used deeper soil water. This concept was used widely in the savanna-related literature (Walker and Noy-Meir 1982, Sarmiento 1984, Eagleson and Segarra 1985) and has been partly supported by root biomass and water use data (Knoop and Walker 1985, Sala et al. 1989, Lee and Lauenroth 1994, Jackson et al. 1996). Trees have been observed to have some deep roots (Eastham and Rose 1990, Stone and Kalisz 1991, Nambiar and Sands 1992), which may make a significant contribution even if their density is low (Stone and Kalisz 1991). Sands and Nambiar (1984) found that the impact of weeds competing for water with neighboring trees decreased as trees grew older and larger. Presumably, the trees were then reaching deep soil layers where water was available, and had become less dependent on water availability in the upper soil layers. Thus, spatial segregation of roots by competing life-forms has been proposed as a means of avoiding competition between trees and grasses while allowing their coexistence.

However, the same field results also documented widely overlapping tree and grass root distributions (Akpo 1993, Belsky 1994, Le Roux et al. 1995, and Mordelet et al. 1997). Ehleringer et al. (1991) showed that herbaceous and woody perennials were using the same water resource and could shift seasonally between possible sources at different depths in the soil profile. Shallow tree roots were reported in West African humid savannas (Lawson et al. 1968, Menaut 1971, Okali et al. 1973) and agroforestry systems, where Jonsson et al. (1988) observed competition for water between trees and intercropped maize with similar rooting patterns. In forest plantations, transpiration by understory vegetation can be large in proportion to the total (Black et al. 1980, Roberts et al. 1980, Price et al. 1986, Black and Kelliher 1989, Kelliher et al. 1990), and the resulting depletion of soil water can cause a reduction in tree growth that can be attributed to competition for water in surface soil layers.

Ecologists have yet to agree that competition for water and the resulting root distributions are the ultimate controls on the relative densities of herbaceous and woody life-forms in savannas. Some have even proposed that savannas have been shaped more by fire and herbivores than by climate (Daubenmire 1968, Ellenberg 1978, Skarpe 1992). Fire controls woody seedling establishment and young tree survival. It is promoted by grass production (fuel load) and its frequency decreases with decreasing rainfall. It enables the rapid release of nutrients from litter and biomass and promotes a postfire flush of young, N-rich grasses, which are very attractive to herbivores. Although browsers also contribute to the reduction in tree growth or even the death of young trees, grazers reduce herbaceous biomass and, thus, fuel buildup and fire frequency, promoting the replacement of grasslands by shrublands. Ellenberg (1978) argued that savannas and sparse tree environments have been created and maintained by grazers. Scholes and Walker (1993) developed the ''disturbance-induced'' coexistence hypothesis that explained how fire, herbivory, and fluctuating rainfall stabilized the precarious mixture of trees and grasses in savannas. Scholes and Archer (1997) explained that, ''since mature trees generally dominate over grasses, . . . all savannas should trend toward a woodland with a sparse understory of grasses,'' unless disturbance keeps the trees under check.

Vegetation dynamics in savannas may thus be explained by two hypotheses. (1) In Walter's (1971) hypothesis of ''niche separation by depth,'' as coined by Scholes and Archer (1997), grasses exploit the upper soil layers, whereas trees have roots both in the upper and the deep soil layers. If there is a large enough difference between shallow and deep water resources and between tree and grass water use efficiencies, both life-forms can coexist. (2) Alternatively, disturbances such as consistent fires, clearing by humans, or grazing by herbivores may be the reason that trees and grasses can coexist (Scholes and Walker 1993, Le Roux et al. 1995). Without disturbance, trees increase their cover at the grasses' expense, slowly shading the grasses and reducing their production. In arid environments, the lack of consistent deep-soil recharge will promote tree dieback and will favor grasses. Frequent and intense fires supported by a vigorous grass growth reduce forest expansion into grassland. Herbivores attracted by the expanse of grasses will contribute to reducing the fuel load and fire frequency, enabling trees to survive.

Increasing carbon dioxide atmospheric concentrations and changes in climate patterns will certainly affect the competitive interactions between grasses and trees. Impacts on water availability will be crucial to the survival or disappearance of savannas. Moreover, enhanced growth caused by release of the carbon source limitation could intensify nutrient limitations, which would affect translocation patterns and resulting root-to-shoot ratios (Allen et al. 1997). It will also affect water use efficiency and alter the competitive balance between trees and grasses, fuel load and fire frequency, and leaf palatability and grazing intensity.

Modeling is one of the few approaches available to test hypotheses about the role of root distribution and fire disturbance on tree and grass competition under historical and future climates. Our model MC1 includes separate vertical root distributions for trees and grasses, thus allowing us to simulate their competition for water at various depths. It also includes a dynamic fire module that estimates fuel load and moisture and simulates

TABLE 1. Interactions among the three modules in MC1: information passed to and from each module.

	Passed to:		
Passed from:	Biogeography	Biogeochemistry	Fire
Biogeography		Position along life-form gradients, which determines interpolation between life-form-specific standard CENTURY parameters	Life-forms (tree leaf type and phenology), used in allometric equations.
Biogeochemistry	Tree and grass leaf carbon.		Aboveground carbon pools. Turnover and decomposition rates from carbon pools. Value of index that modifies primary production as function of available soil moisture.
Fire	LAI and climate smoothing period is reset to zero after occurrence of fire.	Consumption of dead aboveground carbon, associated with losses by gaseous emissions. Nutrient return, calculated as fraction of biomass consumed.	

natural fire events. The model was built to describe the biogeochemical pools and fluxes associated with historical and future changes in global vegetation distribution due to climatic shifts and fire disturbance. It was originally based on the biogeochemical model CENTURY (Parton et al. 1987, 1994) and the biogeography model MAPSS (Neilson 1995). However, only the biogeography rules from MAPSS were retained, whereas CENTURY's biomass and hydrology calculations were conserved and adapted to its new dynamic biogeography driver. MC1 has the advantage of including well-developed belowground processes, but, like many models (Jackson et al. 2000), it is still undergoing development. MC1 simulations must be considered as provisional, awaiting further testing and validation. Many of its current limitations are presented and discussed in this paper.

For this study, we limited the scope of our model applications by assuming that nitrogen was not limiting, by not including grazing, and by keeping CO_2 concentrations constant for both historical and future simulations. Our focus was on the importance of the availability of deep water resources and on the role of fire in maintaining the coexistence of trees and grasses.

This paper begins with a general description of the structure and function of MC1. Methods used to test the hypotheses about the roles of root distribution and fire disturbance on tree and grass competition under historical and future climates are then presented. Results from model simulations for historical and future conditions at Wind Cave National Park are given, followed by an interpretation of the results in light of alternative hypotheses for tree–grass coexistence. Model limitations and their possible implications for the results are also presented. The papers ends with a discussion of the potentially complex effects of future climate and CO_2 changes on tree–grass dynamics at Wind Cave National Park.

DESCRIPTION OF THE MODEL

Overview

MC1 consists of three linked modules simulating biogeography, biogeochemistry, and fire disturbance. A conceptual summary of how the modules interact is shown in Table 1, which summarizes information passed between the modules. The main functions of the biogeography module are to (1) simulate the composition of deciduous/evergreen and needleleaved/broadleaved tree and C_3/C_4 grass life-form mixtures; and (2) classify into different vegetation classes the simulated woody and herbaceous biomass produced by the biogeochemistry module.

The biogeochemistry module simulates monthly carbon and nutrient dynamics for a given ecosystem. Above- and belowground processes are modeled in detail, and include plant production, soil organic matter decomposition, and water and nutrient cycling. Parameterization of this module is based on the life-form composition of the ecosystems, which is updated annually by the biogeography module (Table 1).

The fire module simulates the occurrence, behavior, and effects of severe fire. Allometric equations, keyed to the life-form composition supplied by the biogeography module, are used to convert aboveground biomass to fuel classes (Table 1). Fire effects (i.e., plant mortality and live and dead biomass consumption) are estimated as a function of simulated fire behavior (i.e., fire spread and fire line intensity) and vegetation structure. Fire effects feed back to the biogeochemistry module to adjust levels of various carbon and nutrient pools (Table 1).

TABLE 2. Threshold types and values used to determine the life-form mix in MC1.

Life-form, by gradient	Parameter	Value
Boreal tree gradient (minimum MMT below −15°C)		
DN–DN/EN mix	CI	60°C
DN/EN mix–EN	CI	55°C
Temperate/wet tree gradient (GSP ≥ 55 mm)		
EN–EN/DB mix	minimum MMT	−15°C
Pure DB	minimum MMT	1.5°C
DB/EB mix–EB	minimum MMT	18°C
Temperate/dry tree gradient (GSP < 55 mm)		
EN–EN/EB mix	minimum MMT	1.5°C
EN/EB mix–EB	minimum MMT	18°C
C_3–C_4 grass gradient		
C_3–C_3/C_4 mix	C_3 dominance	66%
C_3/C_4 mix–C_4	C_3 dominance	33%

Note: Abbreviations are as follows: MMT, mean monthly temperature; CI, continentality index (maximum MMT − minimum MMT); GSP, growing season precipitation; D, deciduous; E, evergreen; N, needleleaf; B, broadleaf.

Biogeography

The biogeography module simulates spatial and temporal shifts in the relative dominance of individual life-forms and changes in vegetation classification. The methods used were originally derived from the physiologically based biogeography rules defined in the MAPSS model (Neilson 1995). However, MC1's biogeography module has evolved to more explicitly represent life-form mixtures along dynamic environmental gradients using site production information. The heart of the biogeography module is a life-form interpreter, which delineates continuous gradients of deciduous/evergreen and needleleaf/broadleaf trees and C_3/C_4 grass life-form mixtures as a function of climate. Information from the life-form interpreter (1) forms the basis for categorizing model output vegetation into 17 classes defined by the Vegetation-Ecosystem Modeling and Analysis Project (VEMAP members 1995); and (2) allows for dynamic parameterization of the CENTURY biogeochemistry module. The life-form interpreter and vegetation classification rule bases are presented in this section; dynamic parameterization is discussed in the biogeochemistry module section.

Life-form interpreter.—The life-form interpreter distinguishes four tree life-forms (deciduous needleleaf, DN; evergreen needleleaf, EN; deciduous broadleaf, DB; and evergreen broadleaf, EB) and two grass life-forms (C_3 and C_4) as a function of climate. Shrubs are not explicitly simulated, but are considered short-statured trees. Monthly temperature and precipitation data drive the life-form simulations, which are made on an annual time step. The climatic data are smoothed before they are used by the interpreter to reduce interannual variability in life-form changes, and reflect the lags inherent to plant population dynamics. Each monthly temperature and precipitation value is smoothed with respect to that month's prior values by calculating a running mean of an exponential response curve of the following form:

$$y_t = x_t(e^{-1/\tau}) + y_{t-1}\,[1 - (e^{-1/\tau})] \quad (1)$$

where x_t and y_t are the current month's unsmoothed and smoothed data values, respectively; y_{t-1} is that month's smoothed value calculated for the previous year; and τ is the smoothing period in years. With each simulated fire event, τ is reset to zero and then incremented annually until the next fire event occurs. This procedure mimics the sensitivity of life-form establishment to climate soon after disturbance and the increase in the inertia of life-form composition with greater stand maturity.

Tree life-forms are distinguished in terms of leaf phenology (evergreen vs. deciduous) and leaf shape (needleleaf vs. broadleaf). An environmental gradient algorithm was developed to predict the relative dominance of tree life-forms based on the observed distribution of life-form mixtures along temperature and precipitation gradients across North America.

Heat-limited life-forms are determined through a total annual growing-degree-day (GDD) index (base 0°C). Thresholds are GDD ≤ 50 for ice, 50 < GDD < 735 for tundra, and 735 ≤ GDD < 1330 for taiga.

Trees are assumed to be needle-leaved when the minimum (coldest month) monthly mean temperature (MMT) drops below −15°C, which generally corresponds to daily temperatures at which most temperate broadleaf trees exhibit supercooled intracellular freezing (−41°C to −47°C) as calculated by Prentice et al. (1992) and used by Lenihan and Neilson (1993) and Neilson (1995); see Table 2. Within the needle-leaved zone, the relative dominance of DN vs. EN life-forms is determined by the value of a ''continentality'' index (CI), defined as the difference between the minimum and maximum MMT (Table 2).

When the minimum MMT is >18°C, trees are assumed to be EB. This corresponds to an area of no seasonal frost, following Neilson (1995).

Between the minimum MMTs of −15°C and 18°C,

the relative mixture of the EN, DB, and EB life-forms is determined by both the growing season precipitation (GSP) and the minimum MMT (Table 2). GSP is calculated as the mean monthly precipitation for the three warmest months of the year (month of warmest temperature of the year, averaged with the month before and the month after). This index was originally used by Lenihan and Neilson (1993) and Neilson (1995) to separate broadleaf forests from needleleaf forests, the latter being favored by dry summers. Above a GSP threshold of 55 mm (e.g., eastern United States), the relative mixture of life-forms is defined by the value of a ''wet'' minimum MMT index. A pure DB life-form occurs at a minimum MMT of 1.5°C (Table 2). A mixture of life-forms is linearly interpolated at minimum MMTs between 1.5°C and −15°C (EN–DB mix) and between 1.5°C and 18°C (DB–EB mix); (see Table 2). When the GSP is <55 mm (e.g, western United States), there is no transition through DB life-forms and the relative mixture of the EN and EB life-forms is interpolated along a ''dry'' minimum MMT gradient (Table 2). When the GSP falls between 50 and 55 mm, a linearly interpolated mixture of both wet and dry life-form gradients is calculated.

The relative composition of C_3 and C_4 grasses is simulated using functions from CENTURY, which simulate the potential production of pure C_3 and pure C_4 grass stands from July soil temperature. Soil temperature is estimated from a running average of daily air temperatures interpolated from the monthly temperature values. The ratio of C_3 potential production to the sum of C_3 and C_4 potential production (calculated independently of each other) for the site is used to determine the relative dominance of C_3 grasses (Table 2).

Vegetation classification rule base.—MC1 uses a rule-based approach to simulate the distribution of 17 different vegetation classes defined by the VEMAP project (VEMAP members 1995). Thresholds of maximum monthly tree and grass LAI (leaf area index) are used to distinguish forest, savanna, shrubland, and grassland classes. LAI is calculated from leaf carbon in the biogeochemistry module using the standard CENTURY equations. Vegetation is considered forest at tree LAI ≥3.75 and savanna at tree LAI of 2–3.75. At tree LAI of 1–2, vegetation is classed as shrubland if grass LAI $<$ 1 and as grassland if grass LAI $>$ 1 (Fig. 1). Vegetation is considered grassland if tree LAI $<$ 1. Shrubs are not explicitly simulated, but are considered short-statured trees.

Once the vegetation has been assigned an LAI-based class, specific classes are determined by the life-form mixes calculated by the life-form interpreter and other rules. For example, a savanna with an EN life-form is classed as a temperate coniferous savanna (TCS) (Fig. 1). A CI threshold of 15 is used to distinguish maritime temperate coniferous forest (MTCF) from continental temperate coniferous forest (CTCF), when the life-form mix is EN, DN, or EN–DN mix and the minimum MMT ≥16°C (Fig. 1). A minimum MMT <16°C puts the forest into the boreal coniferous forest (BCF) class.

The percentage of C_3 grasses determines several vegetation classes. Within the shrubland LAI class, the vegetation is classed as temperate arid shrubland (TAS) if the relative composition of C_3 grasses is >55%. A relative C_3 composition of 33–55% is classed as temperate conifer xeromorphic woodland (TCXW), and a C_3 composition of <33% becomes subtropical arid shrubland (SAS). Within the grassland LAI class, a relative composition of C_3 grasses >55% is classed as C_3 grasslands (C_3G) and ≤55% is classed as C_4 grasslands (C_4G).

Biogeochemistry

The biogeochemistry module, consisting of a modified version of CENTURY (Parton et al. 1987), simulates monthly carbon and nutrient dynamics for a combined grass–tree ecosystem. The model includes live shoots (leaves, branches, stems) and roots (fine and coarse), and standing dead material (Fig. 2). It includes perhaps the most detailed representation of soil processes among current biogeochemistry models and has been tested extensively across the globe for terrestrial systems (Parton et al. 1994). Modifications to CENTURY for use in MC1 include a Beer's Law tree–grass shading algorithm, changes to tree and grass vertical root distributions, and the generalization of input parameter sets.

Net primary production.—Forest and grass production are functions of a maximum potential rate modified by scalars representing the effect of soil temperature and of soil moisture on growth. For forests, total production P_t is calculated as:

$$P_t = P_{tg}\, k_t\, k_m\, k_l \tag{2}$$

where P_{tg} is gross tree production (input parameter); k_t and k_m are coefficients that represent the effect of soil temperature and moisture, respectively, on growth; and k_l is a coefficient that relates aboveground wood production to leaf area index.

For grasses, total production P_g is calculated as

$$P_g = P_{gg}\, k_t\, k_m\, k_b\, k_s \tag{3}$$

where P_{gg} is gross grass production (input parameter); k_b is a coefficient that represents the effect of the live/dead biomass ratio on growth, and k_s is a coefficient that represents the effect of shading by trees. We have replaced CENTURY's original light competition function by the Beer's Law formulation (Jarvis and Leverenz 1983).

The production coefficient for soil moisture k_m is defined as

$$k_m = (M_s + M_p)/\mathrm{PET} \tag{4}$$

where M_s is the water available in the soil profile; M_p

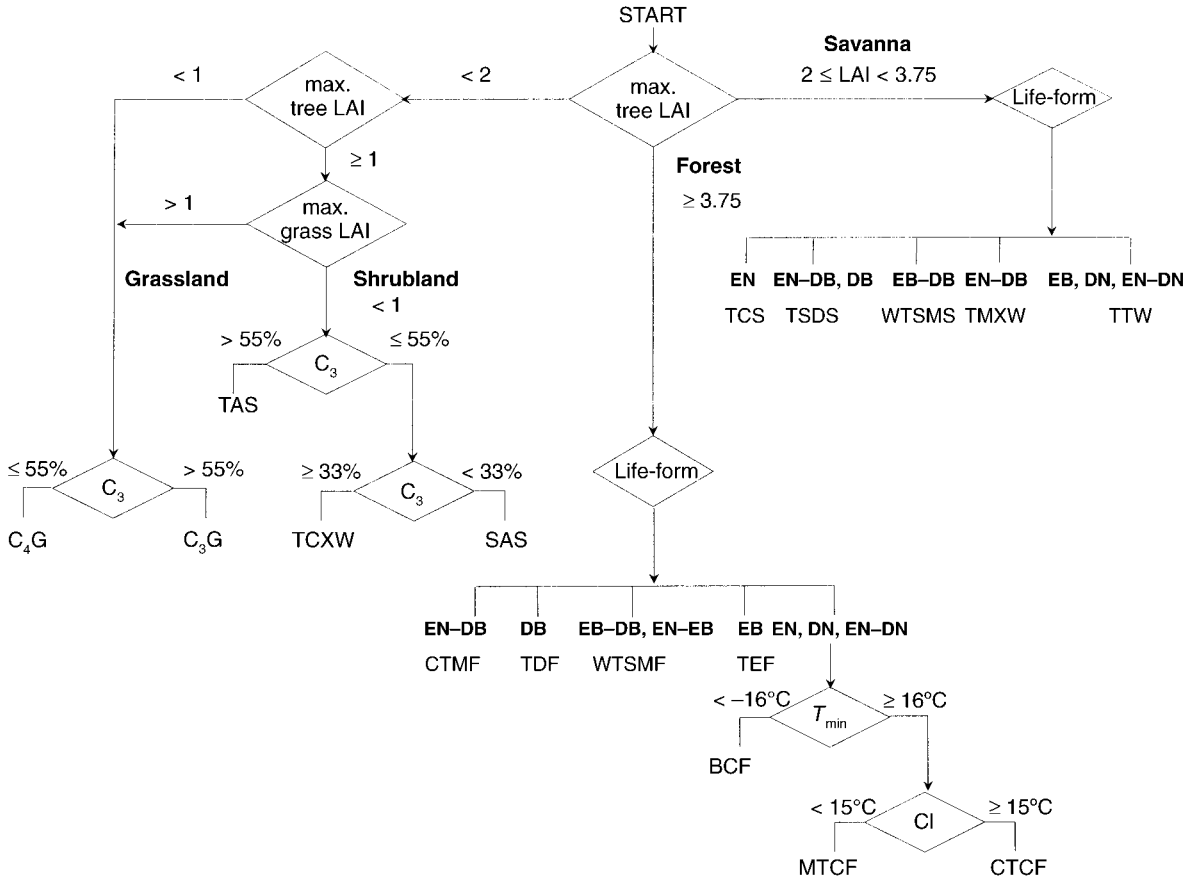

FIG. 1. Schematic of the vegetation classification rule base. Thresholds of maximum monthly tree LAI separate shrublands ($1 \leq$ LAI < 2), savannas ($2 \leq$ LAI < 3.75), and forests (LAI ≥ 3.75). Climatic thresholds (Table 2) are used to determine the life-form associated with each LAI range. Below a tree LAI of 1, the vegetation is restricted to grasslands. Abbreviations: T_{min}, minimum mean monthly temperature (MMT); CI, continentality index (difference between the minimum and maximum MMT); E, evergreen; D, deciduous; N, needleleaf; B, broadleaf; LAI, leaf area index; $\%C_3$ = relative dominance of C_3 grasses. C_4G, C_4 grasslands; C_3G, C_3 grasslands; TCXW, temperate conifer xeromorphic woodland; SAS, subtropical arid shrubland; TAS, temperate arid shrubland; CTMF, cool temperate mixed forest; TDF, temperate deciduous forest; WTSMF, warm temperate subtropical mixed forest; TEF, tropical evergreen forest; BCF, boreal coniferous forest; MTCF, maritime coniferous forest; CTCF, continental temperate coniferous forest; TCS, temperate conifer savanna; TSDS, temperate subtropical deciduous savanna; WTSMS, warm temperate subtropical mixed savanna; TMXW, temperate mixed xeromorphic woodland; TTW, tropical thorn woodland.

is monthly precipitation; and PET is potential evapotranspiration.

The number of soil layers that are assumed to contain the water necessary for plant growth (nlaypg) varies between vegetation types (Fig. 3). The total number of soil layers (nlayer) varies as a function of soil depth and is one of the site-specific model inputs. Available soil water is accumulated in the surface soil layers (nlaypg) for grasses and in the entire soil profile (nlayer) for trees (Fig. 3). The difference in available soil water between grasses and trees corresponds to deep soil water reserves assumed to be accessible only to deep tree roots. This is a modification of the CENTURY configuration, which limited tree water access to the surface soil layers only. In this study, the sensitivity of the model to a change in the accessibility of soil moisture was tested by varying the soil layers available to trees and grasses for water uptake.

Decomposition.—Shoot and root maximum death rates, specific to life-form, are modified by functions of available soil water in the entire profile and the plant root zone, respectively. During senescence, shoot death rate is a fixed fraction of live biomass. Standing dead material is transferred to surface litter at a fall rate specific to life-form. The structural fraction of surface litter and that of belowground litter are further separated into lignin and non-lignin (cellulose, nitrogen-rich compounds) compartments (Fig. 2). Lignin-rich compounds are decomposed directly into the slow organic matter pool, whereas cellulose-rich compounds migrate through the surface or soil microbe (active soil organic matter pool) compartments first. Soil organic

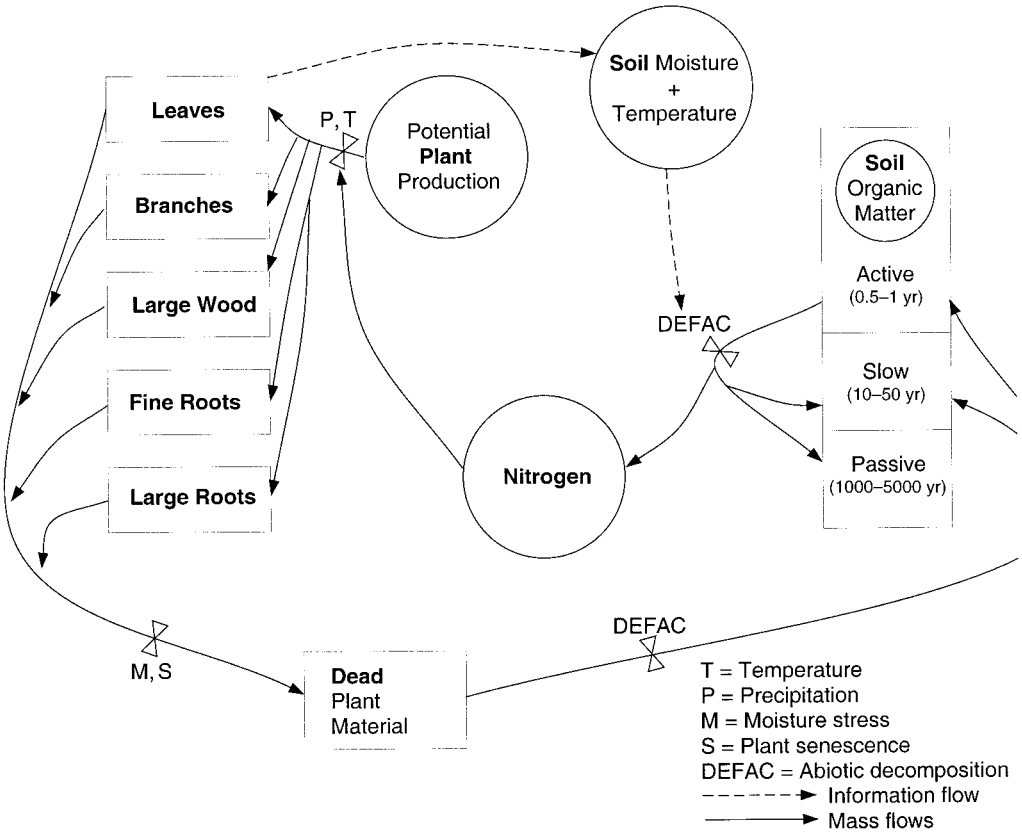

FIG. 2. Schematic of the biogeochemistry module for a woody life-form (adapted from Gilmanov et al. [1997]). Potential plant production is calculated for each life-form as a function of temperature, soil water, and nitrogen availability. Live biomass includes leaves, branches (fine and trunk), and roots (fine and coarse). Grasses are only represented by leaf and root carbon pools. Above- and belowground plant parts senesce as a function of time, drought, and cold stress. Dead leaves and branches accumulate in a surface litter pool, where they are transformed into more slowly decomposing organic carbon. Dead roots accumulate in a belowground litter pool that constitutes the active soil organic matter pool. Decomposition transforms active soil carbon into slow and, finally, passive carbon material. The various soil organic matter pools differ by their turnover times.

matter is divided into three major components: active, slow, and passive (Fig. 2).

Hydrology.—PET is calculated as a function of average monthly maximum and minimum temperatures using the equations of Linacre (1977). Bare-soil water evaporation and interception by the canopy are functions of aboveground biomass, rainfall, and PET. Surface runoff is calculated as 55% of the monthly rainfall when rainfall exceeds 50 mm, and zero when rainfall falls below 50 mm. This rainfall/runoff relationship is based on modeling and empirical analyses in Queensland, Australia (Probert et al. 1995).

Canopy interception, bare-soil water evaporation, and surface runoff are subtracted from monthly precipitation and snowmelt before they are added to the top soil layer. Water is then distributed to the different layers by draining water above field capacity from the top layer to the next layer (Fig. 3). Unsaturated flow is not simulated. Soil layers are 0.15 m thick to a depth of 0.6 m and 0.30 m thick below it. The number of soil layers does not exceed 10. Field capacity and wilting point for the different soil layers are calculated as a function of bulk density, soil texture (inputs to the model), and organic matter content, using Gupta and Larson's (1979) equations. Storm flow is calculated as 60% of the water content of the last soil layer. Water leached below this soil layer is accumulated and lost to base flow.

Transpiration is calculated last as a function of live leaf biomass, rainfall, and PET. The sum of water losses (evaporation, interception, transpiration) does not exceed the PET rate.

Competition for resources.—Grasses and trees compete for light, water, and nitrogen. We have not let soil available N become a growth-limiting factor in this modeling exercise, because no soil N data were available for initializing and calibrating the model. When tree biomass becomes large because of the abundance of soil available water (for example, a high rainfall period with low evaporation potential) and no nitrogen

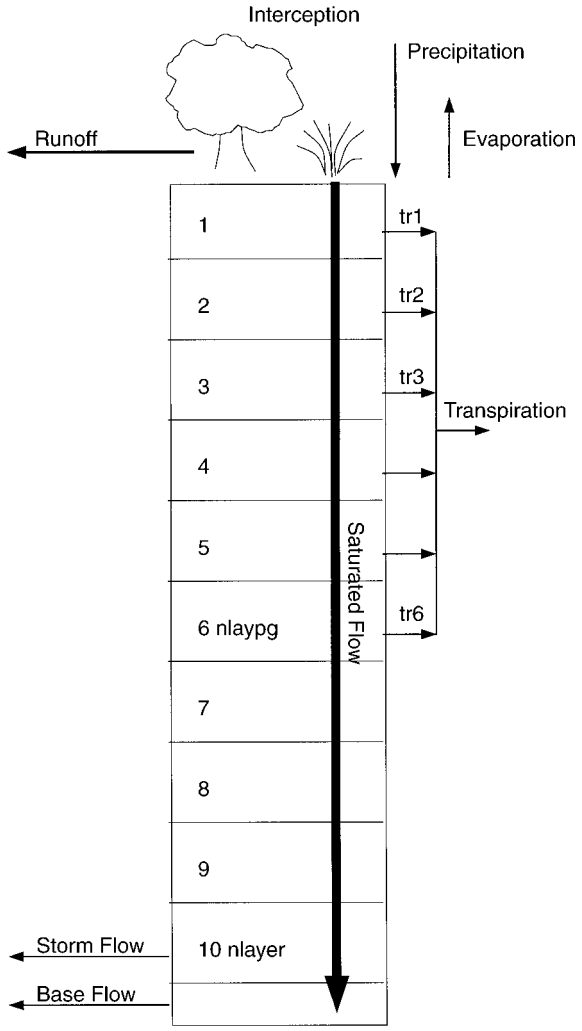

FIG. 3. Hydrologic structure in the biogeochemistry module. Rainfall is intercepted by the life-form canopy. Interception and bare-soil evaporation are calculated as a function of leaf biomass, litter, and standing dead material. Runoff is calculated as a fraction of precipitation. Water infiltrates the soil by saturated flow only. Soil depth (nlayer) is an input to the model. The rooted soil layers are identified as nlaypg, and their depth depends on the vegetation type. Transpiration (tr) is calculated for each rooted soil layer as a function of potential evapotranspiration, leaf biomass, and rainfall. Storm flow is calculated as 60% of the amount of water present in the bottom soil layer. An extra compartment holds the water that does not leave by storm flow or transpiration and is identified as base flow.

limitation, the model reduces grass growth, assuming a shading effect that represents the competition for light between the tree canopy and the grass understory. In the hydrology submodel, the amount of water transpired by plants is calculated as a function of the total plant biomass. There is no life-form-specific calculation of transpiration. Thus, competition for water between trees and grasses occurs through the indirect effect of soil water content on productivity. The production modifier increases for a given life-form if deep soil water resources are available and if the roots of that life-form are present at depth. If deep soil water resources are not available or both life-forms are shallowly rooted, the growth modifier of both life-forms is identical and proportional to the soil water content. In this modeling exercise, the allocation of the deep water resources between life-forms was simply switched to see how production would be affected.

Generalization of input parameters.—CENTURY was designed primarily for site-specific application to individual ecosystems. It uses a parameter set that contains values of tree and grass maximum potential production, temperature growth limits, C/N ratios, leaf turnover rate, soil nutrient concentrations, and related parameters. The parameter set is selected based on an externally supplied ecosystem type, such as a VEMAP vegetation class (VEMAP members 1995). In MC1, however, the ecosystem type may change over time in response to climatic and successional factors. Early applications of MC1 with temporally varying ecosystem types and, hence, temporally varying parameter sets, produced unacceptable discontinuities in predicted carbon pools when the ecosystem type changed. Therefore, a method was developed to reduce the number of parameter sets and to smoothly transition from one set to another.

As discussed previously, the biogeography module calculates climatic indices that describe the life-form composition of an ecosystem as mixtures of deciduous needleleaf (DN), evergreen needleleaf (EN), deciduous broadleaf (DB), and evergreen broadleaf (EB) trees, and C_3 and C_4 grasses. Parameter values appropriate for pure stands of the four tree life-forms and the two grass life-forms were extracted from parameter files that had previously been used with CENTURY (values are listed in Appendix). Linear interpolation between these pure stand values was performed to estimate parameter values for the biogeochemistry module that were appropriate for the life-form mixture predicted by the biogeography module. Transforming CENTURY's static input structure to a smoothly varying, dynamic system resulted in more realistic and natural transitions in model simulations.

Fire

Fire occurrence, behavior, and effects are simulated by the MCFIRE model (Lenihan et al. 1998). The following is a brief description of the overall structure and function of MCFIRE.

Fuel moisture and loading.—Calculations of percentage moisture are made for tree leaves and fine branches, grass leaves, and four size classes of dead fuel (i.e., 1-, 10-, 100-, and 1000-h fuels). The moisture contents of the four dead-fuel classes are estimated using the time lag moisture calculations developed by Fosberg and others (Fosberg 1971, Fosberg and Deem-

ing 1971, Fosberg et al. 1981). For example, a 100-h dead-fuel category corresponds to a particular size class of wood (diameter 1–3 inches; 2.5–7.6 cm) that takes 100 h to come two-thirds of the way toward equilibrium under standard conditions of ambient moisture. Live-fuel moisture is estimated from an index of plant water stress (Howard 1978). The index is a function of the percentage soil moisture simulated by the hydrology algorithms in the biogeochemical module.

MCFIRE estimates the loading in the different fuel classes from carbon in the live and dead aboveground pools simulated by the biogeochemical module. The live grass shoot and live tree leaf pools are summed to estimate the live fine-fuel class load, and the standing dead grass shoot and aboveground grass and tree leaf litter are summed to estimate the dead 1-h fuel class load. A set of allometric equations specific to each lifeform is used to estimate average stand dimensions (i.e., height and bole diameter) from aboveground biomass. The stand dimensions are used in another set of allometric functions to allocate the woody biomass into three different structural components, i.e., fine branches, medium branches, and large branches plus boles (Stanek and State 1978, Means et al. 1994). These three live components, together with live biomass turnover rates and dead biomass decomposition rates from the biogeochemical module, are used to partition the two dead-wood carbon pools into the three dead-fuel classes (i.e., the 10-, 100-, and 100-h dead fuels).

Potential fire behavior and effects.—Surface and crown fire behavior are simulated in MCFIRE as a function of fuel load, fuel moisture, and stand structure. Surface fire behavior is modeled using the Rothermel (1972) fire spread equations, as implemented in the National Fire Danger Rating System (Bradshaw et al. 1983). Crown fire initiation is simulated using van Wagner's (1993) formulation. Indices of fire behavior (e.g., fire line intensity, rate of spread, and the residence time of flaming and smoldering combustion) are used in the simulation of fire effects in terms of plant mortality and fuel consumption (described in the next section).

If a crown fire is initiated in the model, postfire mortality of aboveground live biomass is assumed to be complete. Otherwise, crown mortality is a combined effect of crown scorch and cambial kill simulated in MCFIRE. Crown scorch is a function (Peterson and Ryan 1986) of lethal scorch height (van Wagner 1973) and the average crown height and length as determined by the allometric functions of biomass. Cambial kill is a function of the duration of lethal heat and the bark thickness estimated from average bole diameter (Peterson and Ryan 1986). The percentage mortality of crown biomass is estimated as a function of crown scorch and cambial kill (Peterson and Ryan 1986).

The mortality of live tree roots due to a simulated fire is estimated from the depth of lethal heating in the soil. The depth of lethal heating is modeled as a function of the duration of flaming and glowing combustion at the surface (Peterson and Ryan 1986). The depth vs. duration relationship was derived from empirical data presented by Steward et al. (1990).

Dead-fuel consumption by fire is modeled as functions of the moisture content of the different dead-fuel size classes (Peterson and Ryan 1986). Emissions from fuel consumption are modeled for CO_2, CO, CH_4, and particulate matter as the product of the mass of fuel consumed and emission factors for the different emission gases (Keane et al. 1997).

Fire feedbacks to biogeochemistry.—The standard version of CENTURY (Parton et al. 1987) simulates fire as a scheduled series of fires at one of three levels of intensity. The effects of different levels of fire intensity are defined by parameters that set fractions of the live and dead carbon pools consumed by fire, and fractions of nitrogen and other nutrients returned to the soil. In the initialization phase, MC1 uses the same fire schedule as standard CENTURY and uses the input parameters that define the fractions of live and dead fuel that are consumed by the scheduled fires. In transient mode, however those fractions are simulated by MCFIRE and replace the input parameters (Table 1).

Unlike the standard version of CENTURY, MC1 also simulates live-to-dead carbon pool turnover due to postfire mortality. These equations are included in the biogeochemistry module. In the case of a simulated crown fire, it is assumed that live leaves and branches are completely consumed. Otherwise, live leaves are consumed and live branches are transferred to the appropriate dead carbon pool in proportion to the percentage mortality of the crown. The bole biomass of killed trees or shrubs and the biomass of killed roots are also transferred to dead carbon pools.

Fire occurrence.—The potential fire effects simulated by the model do not feed back to the biogeochemistry module unless MCFIRE determines that a fire has occurred in a given model grid cell. For fire to occur in the model, three different conditions must be met: (1) fuels must be exposed to extended drought, (2) fine dead fuels must be highly flammable, and (3) fire spread must reach a critical rate. Our intent is not to simulate every fire that could potentially occur on a landscape, but rather only the more extensive fires with more significant effects on the vegetation. The moisture content of the 1000-h dead-fuel class is used as an indicator of extended drought. Large, dead fuels are very slow to absorb and release moisture (Fosberg et al. 1981), so their percentage moisture content is a good index of extended periods of either dry or wet conditions.

When the 1000-h fuel moisture drops below a calibrated drought threshold in the model, a simulated fire will occur if there is also a sufficient fine-fuel flammability and fire spread. We use a function from the

National Fire Danger Rating system (Bradshaw et al. 1983) to calculate a probability of flammability and spread. Flammability is a function of fine-fuel moisture and air temperature. The critical rate of spread is a function of the rate of spread estimated by the Rothermel algorithm and a minimum rate of spread for reportable fires (Bradshaw et al. 1983). We use a 50% threshold value of the National Fire Danger Rating system function to determine fire occurrence in our model. Ignition sources (e.g., lightning) are assumed to be always available in this version of the model.

If a fire is triggered in a cell, the simulated fire effects are applied uniformly to the entire cell (50 × 50 m resolution). Currently, there is no provision in MCFIRE for spatially explicit fire spread within and among cells. However, on coarse grids (0.5° of longitude and latitude or greater), only a fraction of a cell is burned.

Fire feedbacks to biogeography.—The fire module calculates changes to carbon and nutrient pools. Fire-caused changes in carbon affect the LAI values that are passed to the biogeography module to help determine vegetation type. The LAI values are smoothed using the same function used for smoothing the climatic values (see Eq. 1). The occurrence of a fire resets the smoothing period to zero, which allows the biogeography rules to predict an open-canopy vegetation type for a few years after a simulated fire (Table 1).

MC1 operation

MC1 is operated in two successive modes: equilibrium and transient. In equilibrium mode, the biogeochemistry module requires an initial vegetation class for parameterization. MAPSS (Neilson 1995) is run on long-term mean climate, which consists of one average year of monthly climate data (usually representing the most recent 30 yr of record). The biogeochemistry module is then run on the MAPSS vegetation class using the same mean climate, until the slow soil carbon pool reaches a steady state. This takes 200–3000 yr, depending on the ecosystem being simulated. Because the fire module cannot be run meaningfully on a mean climate, fire events are scheduled at regular intervals that vary with vegetation type. Grasslands and savannas are assigned 30-yr intervals, whereas certain forests types have fire intervals exceeding 400 yr.

In transient mode, the biogeochemistry module operates on a monthly time step for a period of years, reading the transient climate data and producing estimates of monthly carbon and nutrient pools. The fire module accesses the same climate data and the biogeochemical carbon pools to estimate fuel load and fuel moisture, and maintains a running probability of fire occurrence. If that probability exceeds a certain threshold, a fire is simulated. The fire module then calculates changes to carbon and nutrient pools, which are passed back to the biogeochemistry module for use in the following month of operation (Table 1). Emissions from the simulated fire are also calculated. Every year, the biogeography module uses climate data and maximum monthly tree and grass LAI (derived from standing biomass data from the biogeochemistry module) that have been smoothed to reduce interannual variability. When a fire has occurred, the LAI smoothing period is reset to zero, thus allowing the vegetation classifier to simulate a period of low-cover vegetation following the fire (Table 1). Vegetation classification is thus allowed to proceed through a series of successional stages, e.g., from grassland to savanna to forest. The appropriate life-form composition is determined each year to start the next simulation year. The life-form mixture is used by the fire module for allometric calculations, and by the biogeochemistry module to determine life-form-dependent parameter values (Table 1).

METHODS

Study area

The study area is a 12.5-km^2 section of Wind Cave National Park (WCNP) in the Black Hills of South Dakota, USA (Fig. 4), including 5000 grid cells (50 × 50 m resolution). The implementation of MC1 at WCNP is part of a larger study to assess the impact of global change on the Central Grasslands Region at landscape to regional scales (Neilson et al. 1996). WCNP is an excellent test site for the present project because of the diversity of plant communities and the availability of model input data sets. The topographic setting is of relatively flat upland terrain interspersed with hills and occasionally divided by stream channels. Elevations range from 1290 to 1530 m.

The WCNP landscape includes several of the Central Grassland vegetation types simulated by MC1, including temperate evergreen conifer forest and savanna at higher elevations and on north-facing slopes, C_3 and C_4 grasslands in lowland areas, and deciduous hardwoods in riparian/wetter zones. The distribution of forest and grassland communities appears to be determined by a combination of soil texture and moisture conditions, as well as fire and grazing regimes.

Input data

MC1 requires gridded maps of soil texture (i.e., percentage sand, silt, and clay), rock fraction, and depth to bedrock. It also requires a gridded, monthly climate data set of precipitation, minimum and maximum temperature, vapor pressure, wind speed, and solar radiation. Two climate data sets were prepared: (1) an historical time series (1895–1994); and (2) a future climate scenario (1995–2094) based on Hadley Center GCM (General Circulation Model) predictions for the next century (Jones et al. 1997). Methods used to develop these data sets incorporated the relationships between landform type and soil depth and texture, and the effects of elevation and topographic ex-

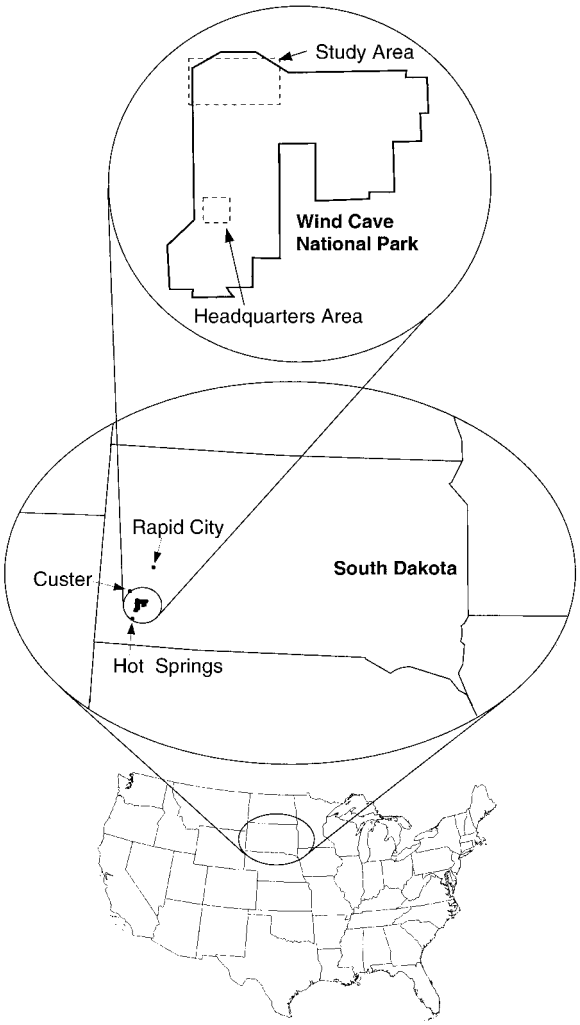

FIG. 4. Location of Wind Cave National Park, South Dakota, USA, and of the study area.

posure on local climate. These methods are detailed in Appendix A.

Experimental design

As discussed previously, the standard rooting configuration for the MC1 biogeochemistry module is to allow trees to access water from all soil layers in the soil profile (nlayer), but to restrict grass access to only the surface soil layers (nlaypg) (Fig. 3). This tree deep/grass shallow (TDGS; Table 3) configuration also corresponds to Walter's (1971) hypothesis of deeply rooted trees vs. shallowly rooted grasses in savannas, which is widely accepted in the literature. This scheme was modified systematically to test the sensitivity of the model to alternative water uptake configurations for all combinations of tree and grass roots being shallow or deep (Table 3).

For each of the rooting configurations, MC1 was run in equilibrium mode using a 1961–1990 mean climate to produce steady-state carbon pools, then in transient mode on the 1895–1994 climate time series. For the climate change scenario, MC1 was run (1) in equilibrium mode as just described, then (2) in transient mode for 200 yr using two cycles of a detrended 1895–1994 climate data set to obtain a reasonable dynamic fire frequency; and finally (3) in transient mode for the simulated 1995–2094 climate time series. (See Appendix A for a discussion of the climate data sets.)

The biogeochemistry module was configured to allow a tree–grass mixture (CENTURY savanna mode), and no grazing was scheduled. N demand was always met for the purpose of this exercise and was never limited by local conditions (which were unknown because no soil N data have been collected at the site). CO_2 concentrations were kept at a constant 350 ppm for both historical and future simulations.

RESULTS

Historical climate

The first half of the 20th century was generally wetter than the second half at Wind Cave National Park (Fig. 5). Because water was readily available for growth, simulated tree biomass was high (up to 3000 g C m^{-2}) from 1894 until 1936, when a large simulated fire during the 1930s drought consumed most of the woody biomass (Fig. 6a). Temperatures were above average from 1930 to 1940 (Fig. 5), which caused a drying of fuels and resulted in three fires in rapid succession (1931, 1936, and 1939). Trees never recovered after the 1930s, because the simulated fire frequency increased, with five large fires in the next 40 yr (1954, 1960, 1966, 1974, and 1985), mainly as a consequence of fuel load increases in the form of grass biomass (Fig. 6a) and occasionally higher temperatures. A fire during the 1950s' drought affected grass biomass to a larger extent than did subsequent fires. At that time, woody

TABLE 3. Rooting depth sensitivity tests performed with MC1.

Configuration	Description	Soil depth rooted by trees (m)	Soil depth rooted by grasses (m)
TDGS (standard)	trees deep; grasses shallow	1–1.5†	0.3
TDGD	trees deep; grasses deep	1–1.5†	1–1.5†
TSGS	trees shallow; grasses shallow	0.3	0.3
TSGD	trees shallow; grasses deep	0.3	1–1.5†

† Varies with soil depth: ~1 m on ridgetops to ~1.5 m in lowlands.

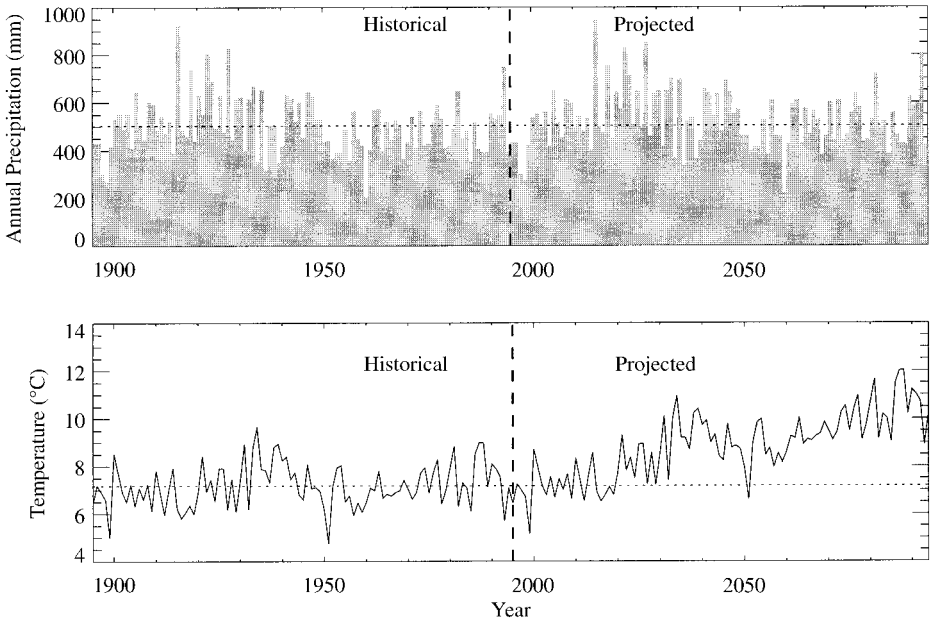

FIG. 5. Historical (1895–1994) and estimated future (1995–2094) annual average temperature and total annual average precipitation over the study area in the northwest corner of Wind Cave National Park, South Dakota, USA. For these graphs, temperature and rainfall were averaged for the 5000 grid cells included in the study area.

biomass was increasing (~1000 g C/m^{-2}) and the fire consumption was large, even though the number of grid cells affected by the fire was not as large as in later fires (Fig. 6a).

When trees are deeply rooted (TDGS and TDGD, Table 4), simulated tree NPP and biomass are greater and grass NPP and biomass are lower than when they are shallowly rooted (TSGS and TSGD, Table 4). Because tree leaf biomass in the deeply rooted tree scenarios is at least twice as large as in the shallowly rooted tree scenarios, the difference in grass growth can be explained, in part, by the shading effect of trees over grasses (see *Discussion*). Grass biomass is greatest when trees are shallowly rooted and grasses are deeply rooted (Fig. 6d). Tree biomass is reduced by >60% when trees are shallowly rooted (Fig. 6b, d).

Soil carbon pools are smaller when grasses are shallowly rooted (TDGS and TSGS, Table 4) than when they are deeply rooted. When grasses are deeply rooted, their root biomass increases by ~30% (Table 4). This large C pool and its turnover contribute to the greater size of the soil C pool.

Fire return intervals are longer for deeply rooted tree configurations because grass biomass is lower and, thus, the fuel load is reduced. Similarly, when grass biomass is lower in shallowly rooted grass scenarios (TDGS and TSGS), the fire return intervals are greater (Table 4). The frequency and the number of grid cells that experience fire are greater when trees are shallowly rooted (Fig. 6b, d), in comparison to the TDGS configuration. Simulated C releases from fires vary from 46 to 53 g C·m^{-2}·yr^{-1} across all root configurations (Table 4). This is in good agreement with Mack et al. (1996), who estimated mean annual carbon emissions by vegetation fires for the northern United States at ~50 g C·m^{-2}·y^{-1}.

Climate change scenario

The 1995–2094 scenario for climate change shows a slight increase in precipitation and a large increase in temperature (Fig. 5). Interdecadal changes in plant biomass are very similar to those obtained using the historical climate (not shown here); tree biomass is high until the mid-2030s, then drops precipitously due

→

FIG. 6. (a) Simulated total tree and grass biomass (g C/m^2) over our study area. Five thousand grid cells were averaged for each year between 1895 and 1994. The date and the extent (number of grid cells that sustained a fire) of simulated natural fires are also presented. Trees were assumed to be deeply rooted, whereas grasses were shallowly rooted (TDGS). Simulated relative differences between tree and grass biomass are given for three root configurations other than the standard TDGS root configuration: (b) TSGS; (c) TDGD; and (d) TSGD. The relative difference was calculated as: ([(T*x*G*y* biomass − TDGS biomass]/TDGS biomass). Also presented is the absolute difference in the number of grid cells that sustained a fire between each rooting configuration and TDGS. Negative solid bars correspond to missing fires (which existed with the TDGS configuration); positive solid bars correspond to new fires (which did not exist with the TDGS configuration).

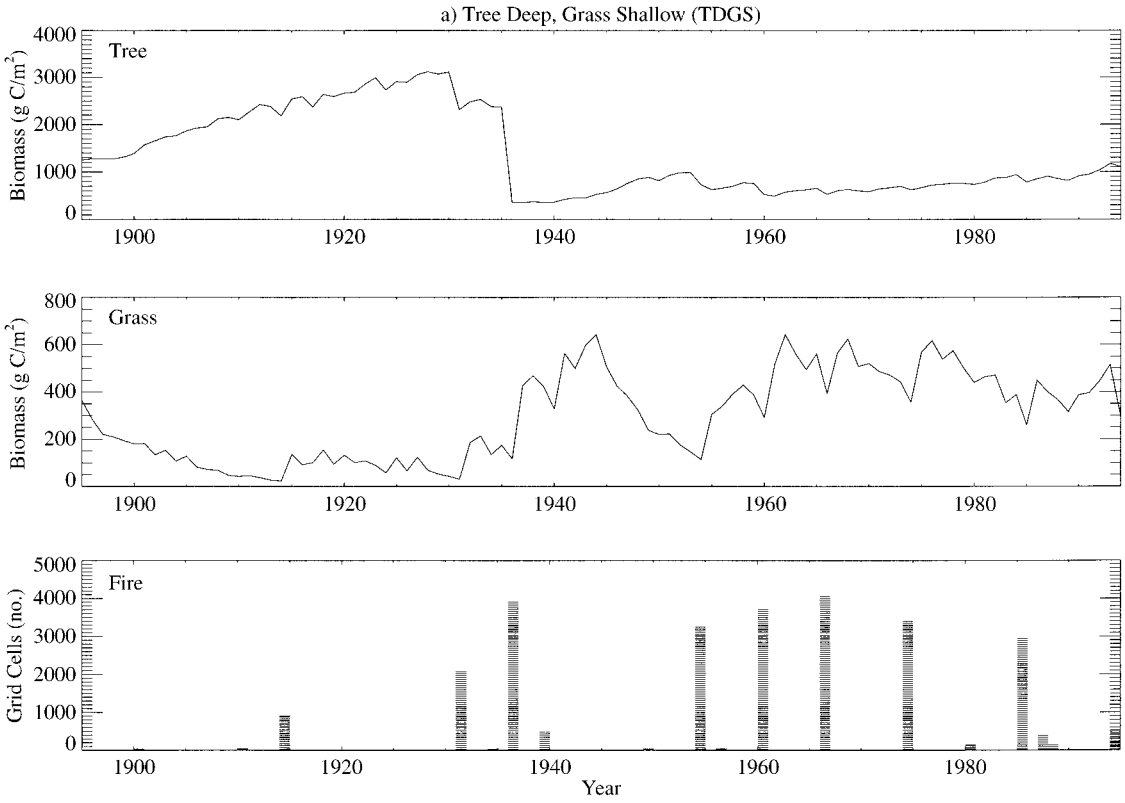
a) Tree Deep, Grass Shallow (TDGS)
Tree
Biomass (g C/m^2)
Grass
Fire
Grid Cells (no.)
Year

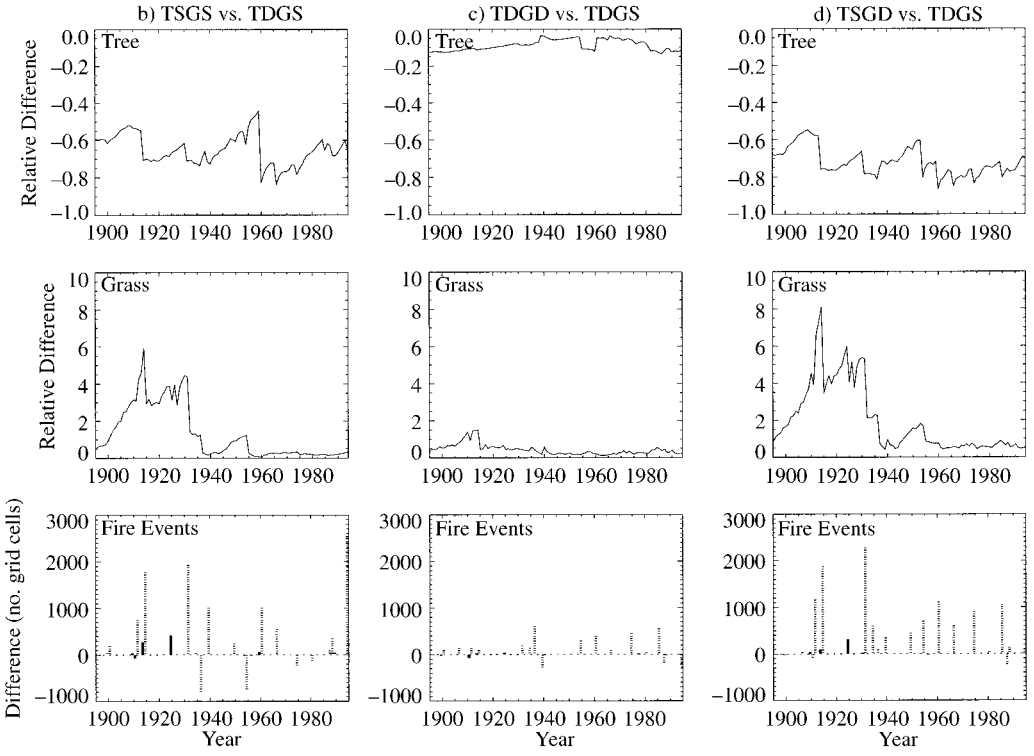
b) TSGS vs. TDGS
c) TDGD vs. TDGS
d) TSGD vs. TDGS
Tree
Grass
Fire Events
Relative Difference
Difference (no. grid cells)
Year

TABLE 4. Summary statistics of MC1 rooting depth configurations for historical climate. Values are means for the 100-yr period for all pixels. Biomass and production values are divided into trees (T) and grasses (G).

Variable	Life-form	TDGS	TDGD	TSGS	TSGD
Biogeochemistry					
Net primary production (g C/m^2)	T	178	162	88	75
	G	136	180	211	277
Live leaf biomass (g C/m^2)	T	164	148	76	63
	G	42	52	66	81
Total root biomass (g C/m^2)	T	198	179	90	75
	G	255	336	400	520
Total biomass (g C/m^2)	T	1345	1216	480	395
	G	297	389	466	601
Total biomass C/N ratio	T	223	222	180	176
	G	44	41	41	41
Surface soil mineral nitrogen (g N/m^2)		14	11	10	6
Total soil organic matter (g C/m^2)		7902	8334	7611	8366
Soil organic matter C/N ratio		11.3	11.5	11.0	11.5
Hydrology					
Soil moisture, surface (cm)		0.03	0.03	0.04	0.04
Soil moisture, surface + deep (cm)		0.16	0.16	0.20	0.21
Fire					
Fire return interval (yr)		20	17	14	13
Emissions (g C·m^{-2}·yr^{-1})		46	50	48	53

Note: See Table 3 for definitions of rooting configurations.

to drought-induced fire; grass increases in response to the lowered tree biomass. This similarity in behavior is due to the use of 1895–1994 climate as the basis for the climate change scenario (see Appendix A for details). Overall, future tree biomass is lower compared to 1895–1994, whereas grass biomass is generally higher, especially in the early part of the century (Fig. 7, Table 5). The exception is the TSGD configuration, in which grass biomass is slightly lower than for the same configuration during historical period (Fig. 7d). Because NPP and biomass increase for grasses (except for TSGD) and decrease for trees in comparison to the historical climate results, the fire return interval decreases (Fig. 7). Total soil organic matter decreases in the future scenario (Table 5).

Differences in results due to the climate change scenario are small compared to those caused by the various rooting configurations (Table 5). The ranges in NPP, biomass, and other ecosystem properties across the four rooting configurations are typically several times those of the differences in mean values between the historical and future scenario. However, differences between early- and late-century results are quite large, sometimes approaching the magnitude of the ranges across rooting configurations (Table 5).

Maps of WCNP observed vegetation distribution, MC1 simulated vegetation (TDGS) with historical climate data, and MC1 simulated vegetation (TDGS) with the climate change scenario are shown in Fig. 8. The maps correspond to the state of the vegetation one year following a large fire event. Vegetation types were pooled together into three categories: forest, savannas, and grasslands, to simplify visualization. MC1 overestimated the extent of forested area. However, the spatial arrangement of vegetation types remains consistent with the observed pattern. The large patch of savanna in the northwest corner of the study site corresponds to an area that was not burned the previous year. MC1 predicts a decrease in the extent of forests with the climate change scenario in comparison to the historical climate, but it also predicts a large decrease in the extent of savannas. Changes in vegetation types are dynamic due to the occurrence of fire events and, thus, are difficult to display. Results shown here represent only a snapshot of the period studied.

→

FIG. 7. Simulated changes in tree and grass total biomass, and the date and extent of natural fires during the simulated HadS climate scenario (1995–2094) period for the four root configurations: (a) HadS TDGS vs. historical TDGS; (b) HadS TSGS vs. historical TDGS; (c) HadS TDGD vs. historical TDGD; and (d) HadS TSGD vs. historical TSGD. Relative differences between HadS and historical climates were calculated as: ([(HadS − historical]/historical). Fire histograms represent the absolute difference between HadS and historical climates in the number of grid cells that sustained a fire. Negative solid bars correspond to missing fires (which existed with the historical, but not the future climate scenario); positive solid bars correspond to new fires (which did not exist with the historical climate scenario).

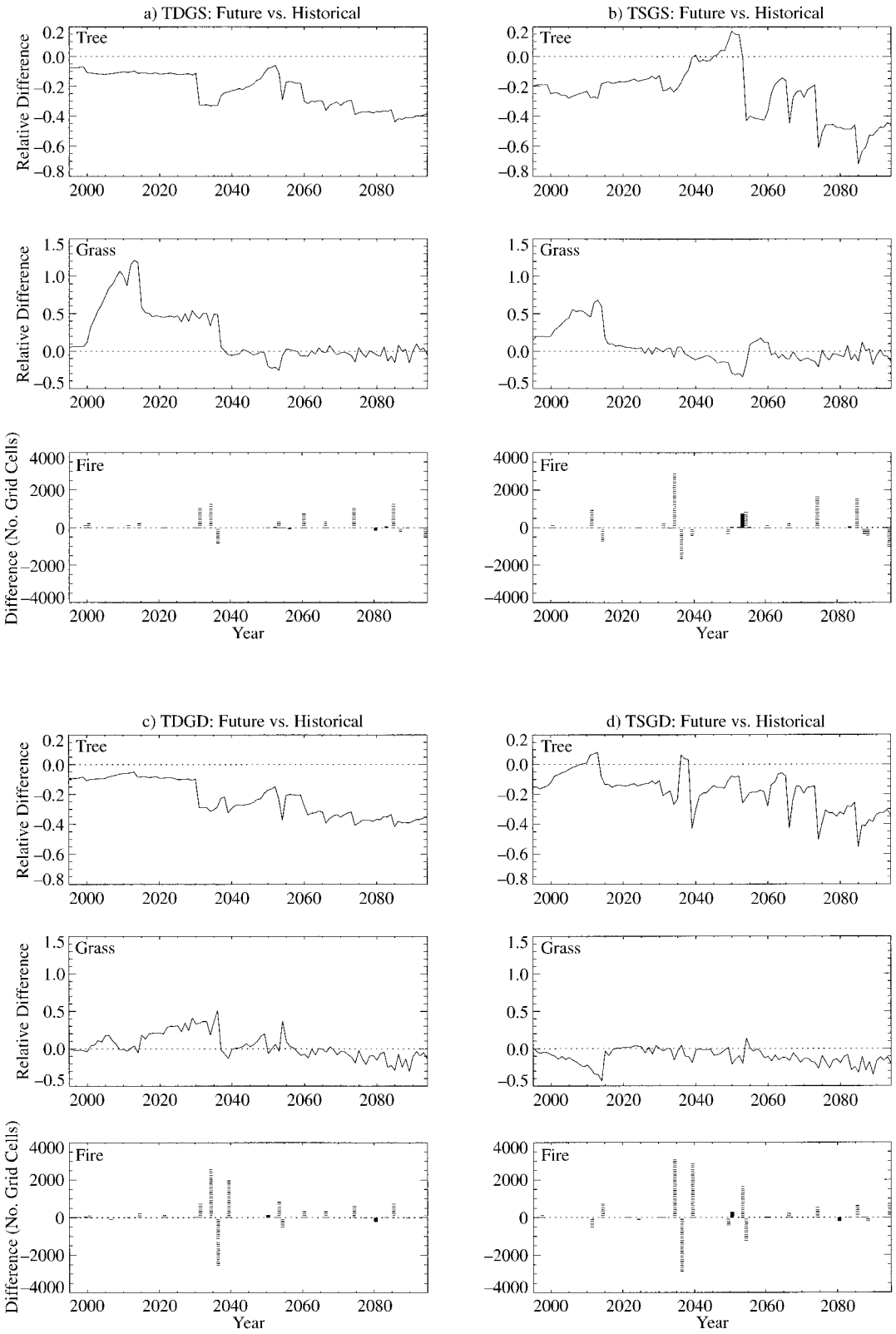
a) TDGS: Future vs. Historical
b) TSGS: Future vs. Historical
c) TDGD: Future vs. Historical
d) TSGD: Future vs. Historical
Tree
Grass
Fire
Relative Difference
Difference (No. Grid Cells)
Year
2000
2020
2040
2060
2080

TABLE 5. Comparison of early- and late-century MC1 statistics for the historical and Hadley Center sulfate aerosol (HadS) scenarios.

Variable	Life-form	Early century				Late century			
		Historical		HadS		Historical		HadS	
		Mean	Range	Mean	Range	Mean	Range	Mean	Range
Biogeochemistry									
Net primary production (g C m^2)	T	222	130	208	136	76	67	50	37
	G	66	93	79	102	274	135	294	93
Live leaf biomass (g C/m^2)	T	206	137	190	138	65	62	41	34
	G	21	28	25	32	83	34	86	21
Total root biomass (g C/m^2)	T	220	150	201	147	78	78	51	46
	G	153	193	179	206	527	248	457	140
Total biomass (g C/m^2)	T	1444	1238	1295	1175	479	588	297	361
	G	174	221	204	238	610	281	543	161
Total biomass C/N ratio	T	196	37	190	45	190	75	178	78
	G	41	1	41	1	41	2	41	1
Surface soil mineral nitrogen (g N/m^2)		14	6	13	5	6	9	5	6
Total soil organic matter (g C/m^2)		8170	718	8065	829	8076	898	7897	796
Soil organic matter C/N ratio		11	0	11	0	11	1	11	0
Hydrology									
Soil moisture at surface (cm)		0.01	0.02	0.06	0.04	0.04	0.02	0.05	0.01
Soil moisture, surface + deep (cm)		0.07	0.06	0.09	0.11	0.08	0.04	0.07	0.01

Notes: Early century refers to the period 1905–1914 for historical and 2005–2014 for HadS. Late century is 1975–1984 for historical and 2075–2084 for HadS. For these 10-yr periods, the reported means were calculated by averaging values over all 5000 pixels for each rooting-depth configuration and then averaging these means. Reported ranges represent the range of 5000-pixel means over the four rooting depth configurations. Biomass and production values are divided by life-form into trees (T) and grasses (G).

DISCUSSION

Competition for resources

Results show that the model is clearly sensitive to the allocation of deep water resources. When trees are deeply rooted, fire is the only factor that will allow grasses to grow. Without fire, trees become the dominant life-form. The allocation of deep water to trees gives them a competitive advantage over grasses. This simple representation of belowground resource competition contradicts Walter's (1971) hypothesis that trees and grasses coexist because they do not access the same water sources. In this case, because tree potential production is greater than that of the grasses, and given a nonlimiting source of nitrogen, trees develop aboveground biomass faster than do grasses and reduce their development by shading them. Mordelet and Menaut (1995) documented that light interception

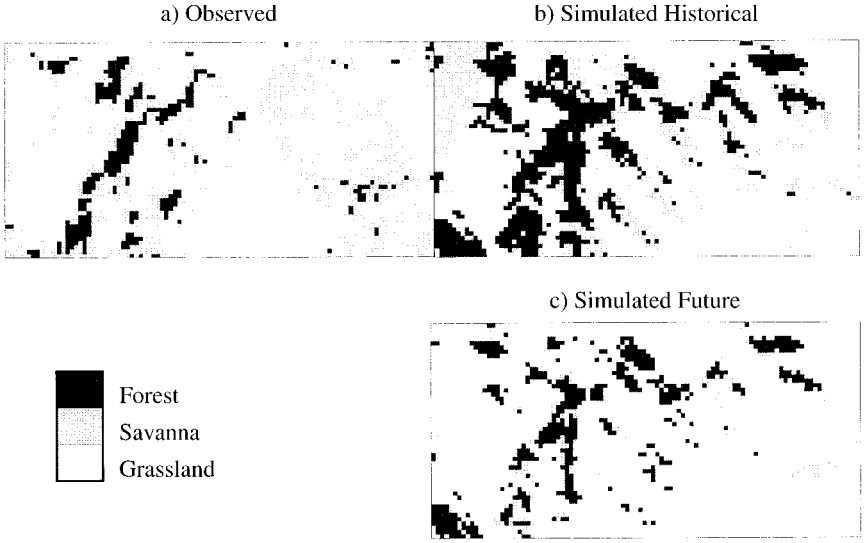

FIG. 8. Vegetation distribution at the study site in Wind Cave National Park: (a) observed; (b) simulated historical; and (c) simulated HadS climate scenario. Both simulated maps are from the TDGS configuration (deeply rooted trees, shallowly rooted grasses). Vegetation types were simplified and pooled into three categories: forests, savannas, and grasslands.

is the most important factor in reducing grass growth under trees, despite soil enrichment by tree litter. In results not shown here, we tested the model for a limited nitrogen source and the trees still managed to outcompete grasses. Not only do trees gain an advantage by accessing deep water reserves, but also N uptake for each life-form is simulated as a function of their net primary production. By having access to deep soil water, trees reduce the water constraint on their production and can thus outgrow grasses.

This result supports Daubenmire's (1968) statement that fire has always been used to ''maintain grass dominance in environments where, in its absence, woody vegetation would overwhelm grass.'' A look at the simulated historical trace of tree and grass biomass (Fig. 6a) shows that trees clearly dominate over grasses in the first part of the century, when precipitation is abundant. However, drought conditions are a cause of death for the trees. Canopy opening reduces the simulated shading effect and contributes to a significant increase in grass biomass. More frequent fires are keeping the tree biomass under check in the latter part of the century, when grass biomass and, thus, fuel load, remain high. When fire is prevented in the model, trees dominate the entire period of record (data not shown here). In reality, wildfire suppression occurred in 1898 at Wind Cave National Park and pine encroachment in the forest–grassland ecotone was reported by the locals (Gartner and Thompson 1972). The park management had to start a prescribed fire program to limit forest expansion and maintain the grazing range for native herbivores.

When trees are simulated as being shallowly rooted, their competitive advantage disappears and grass biomass increases significantly. Without deep soil water, tree production and biomass are reduced, thus allowing for greater grass growth. Only when both life-forms share the same water resource is tree growth reduced enough to allow grasses to grow. This is supported by Ehleringer et al. (1991) and Le Roux et al. (1995), who observed the overlap of tree and grass vertical root distributions and their sharing of the same water source. Le Roux et al. (1995) also reported that savanna trees competed with herbaceous species more intensively at wetter sites and that disturbance was the most important factor preventing the trees from outcompeting the grasses in those wet environments. Ehleringer et al. (1991) came to the conclusion that if the climate were to become drier, especially during the summer, herbaceous vegetation would be a more successful competitor.

Any single-factor hypothesis of savanna structure for WCNP is likely to be incomplete. Climate sets the stage with low and variable rainfall and relatively high water demand. Different rooting depths allow competition where roots overlap (e.g., humid savannas), but also foster coexistence due to some niche separation (e.g., drier savannas). Feedbacks exist whereby water uptake by deep roots helps to produce more tree leaf area, thus shading grasses and further enhancing tree competition for water in surface layers. With climate variation, rainfall may not reach deep layers in dry years, hindering trees and favoring grasses. Fires fueled by high grass biomass will further diminish the trees and favor grass growth. Clearly, our model addresses some of these issues and constitutes a useful tool to provisionally test the various hypotheses that explain the coexistence of trees and grasses.

Model sensitivity and limitations

MC1 is still being modified and is a work in progress. Future enhancements will include a modification of the hydrology submodel. In this study, production of the various life-forms simulated by MC1 varied greatly with availability of deep soil water (Table 4). Consequently, we would like to more accurately simulate the transport of water down the soil profile. In the original CENTURY version, unsaturated flow was not included in the water balance. We intend to introduce this flow into the next version of the model, using equations from MAPSS (Neilson 1995). Similarly, we intend to add the MAPSS equations used to calculate runoff as a function of soil saturation. (Validating simulated runoff and base flow is problematic at Wind Cave National Park because an unknown amount of water is lost through underground caverns and thus escapes conventional streamflow measurement.) We also plan to calculate separately the amount of water transpired by each life-form to better simulate the competition between grasses and trees. A water availability scalar specific to life-form will then be carried over to modify potential production. The current configuration allows changes only to the allocation of deep water between trees and grasses. In certain sites, the number of upper soil layers, which is determined by the vegetation type, is identical to the total number of soil layers at that site, and thus does not allow for the existence of deep soil water reserves. Several equations that would more clearly represent belowground competition of the life-forms are being tested.

In equilibrium mode, the standard CENTURY fire schedule is used and biomass reductions occur at regular intervals in the development of the various ecosystems. For example, in many forest ecosystems, standard CENTURY assumes that a fire occurs every 200 yr. The 200-yr periods of regrowth allow the systems to slowly build up their carbon and nutrient pools and attain the same vegetation type that existed before the occurrence of the fire. The dynamic fire model that we use in transient mode affects vegetation dynamics more dramatically. In transient mode, if the climate of the particular site where the forest exists is sufficiently moist, trees will develop a closed canopy and will prevent the development of grasses. Even in the event of

a drought, the fine-fuel load (amount of dead grasses) may not be sufficient to trigger a fire in this older forest. Therefore, it is difficult to dynamically simulate succession from closed-canopy forest to grassland. In this situation, prescribed fire is relied upon to simulate not only tree mortality due to disturbance, but also noncatastrophic dieback of the woody vegetation.

In general, the model is very sensitive to changes in the values of CENTURY parameters that were originally chosen from representative stands across the United States (Bill Pulliam, *personal communication*). Production levels vary greatly between deciduous forests and evergreen forests, and the standard CENTURY parameters associated with deciduous trees make them poor competitors compared to evergreen trees (Appendix 2, Table 2.1). For example, deciduous klai, which relates LAI to large wood biomass, is only half of that of the evergreen klai. In addition, all deciduous leaf biomass drops each year, and therefore does not have the potential to build up a dense, grass-shading canopy as quickly as does evergreen leaf biomass. In the life-form interpreter, the choice between eastern deciduous forests and western evergreen forests is based on a threshold GSP. The GSP gradient is steep across the Great Plains, and Wind Cave National Park is located near the threshold GSP. For these simulations, we adjusted the GSP threshold to produce the mainly evergreen vegetation occurring there. Regional validation exercises are planned to further refine the location and sensitivity of the GSP threshold across the Great Plains in the context of VEMAP, (the Vegetation–Ecosystem Modeling and Analysis Project) (VEMAP members 1995).

The climatic data and maximum tree and grass LAIs are smoothed before they are used by the life-form interpreter to reduce interannual variability in life-form changes and to reflect the lags inherent to plant population dynamics. The maximum period over which smoothing can occur is currently 10 years. A maximum smoothing period of 50 years was used initially, but was found to give too much inertia to the system and did not reflect the profound effects of fire disturbance and the advent of new vegetation types. However, more sensitivity analyses are necessary to determine if 10 years indeed corresponds to the ideal maximum smoothing period for a variety of vegetation types.

Grazing, which is available in MC1, but was not examined in this paper, would tend to reduce grasses and their roles as fire promoters and water competitors. The simulated drop in tree biomass during the Dust Bowl period of the 1930s (Fig. 6a) assumed an ungrazed landscape, but in actuality, heavy grazing was occurring in the area. Grazing may have removed enough grass biomass to significantly reduce the occurrence and intensity of fires, allowing the continued dominance of trees over grasses. On the other hand, grazers can reduce tree density by feeding on tree seedlings, but few data exist on the impact of grazers on tree development. MC1 applications are now being performed at WCNP to study the interactions of climate change and variability with management influences such as grazing and prescribed fire.

Due to a lack of soil nitrogen data, we did not allow the model to simulate nitrogen limitations. Moreover, rates of nitrogen fixation and deposition (input parameters) are poorly known. This clearly biased the results. We are now testing the model with various levels of soil nitrogen and are calculating the impacts of the initial size of the soil nitrogen pool on vegetation dynamics.

Future climate

The climate change scenario examined in this paper produced a number of complex ecosystem responses on the WCNP landscape. The warmer, but only slightly wetter, than historical scenario produced a general reduction in tree biomass, an increase in grass biomass, a reduction in soil organic carbon, and more frequent but smaller fires. The distributions of both closed forests and open savannas were substantially reduced and the extent of grasslands increased. These combined changes would produce a net release of carbon from the landscape to the atmosphere. The biogeographic shifts would alter wildlife habitat availability and biodiversity within the landscape.

Changes in the size of biogeochemical pools produced by the climate scenario were overwhelmed by the range of response across the four rooting configurations, indicating that MC1 is highly sensitive to the specification of belowground processes. Belowground data suitable for calibration and validation of existing models are typically limited. Fortunately, recently published results (Stone and Kalisz 1991, Canadell et al. 1996, Jackson et al. 1996, 1997, Vogt et al. 1996) are beginning to provide enough baseline information to build large-scale dynamic vegetation models with a more accurate description of belowground biomass. These models can then be used to address such issues as the role of deep roots in carbon sequestration. Deep roots are a potentially significant carbon source to soil organic matter pools (Canadell et al. 1996) and deep carbon pools could be an important factor in the missing carbon sink (Jobbágy and Jackson 2000, Trumbore 2000). The impact of climate change on carbon allocation to the roots and on belowground resource availability needs to be seriously examined, with models being used as tools to expand on preliminary laboratory or field results and to test new hypotheses.

The drought of the 1930s lasted about seven years; in its worst year, almost 70% of the United States experienced severe or extreme drought conditions. The drought of the 1950s lasted five years and covered much of southern and central Great Plains. Were these droughts part of a naturally varying climate and will

they continue to occur on a periodic basis, or are they exceptional events? Instrumental records are too short to answer such questions. However, paleoclimatic records show that similar events have occurred periodically since the 1300s and generally have lasted <10 years (David Rind, *personal communication*). As concentrations of greenhouse gases continue to increase in the atmosphere, precipitation, derived primarily from ocean surface evaporation, is not expected to increase as rapidly as evaporation from land, because oceans should warm more slowly than the land surface. Therefore, increased drought frequencies and intensities are anticipated in a future warmer world. Ehleringer et al. (1991) support the hypothesis that if summer rainfall decreases in the southwestern deserts of North America, herbaceous perennials, which have a competitive advantage over woody perennials (except for phreatophytes like mesquite) in using summer precipitation, could outcompete them in a warmer world. In our simulation, the decrease in precipitation in the second part of our century favored the growth of grasses. This tendency is similar to the one that we simulated for the 21st century using the Hadley Center scenario. Thus, our simulations would agree with the Ehleringer et al. (1991) suggestion that the future might see more abundant grasslands in the arid lands of North America. This should bear important consequence with regard to the management of National Parks such as Wind Cave, which is situated at the ecotone between grasslands and forests.

Acknowledgments

We thank Ray Drapek for preparing the future climatic scenario and for generating most of the figures presented in this paper. This work was funded, in part, by the U.S. Department of Energy, National Institute for Global Environmental Change, Great Plains Region (LWT 62-123-06509); the U.S. Geological Survey, Biological Resources Division, Global Change Program (CA-1268-1-9014-10); and the USDA-Forest Service, PNW, NE, SE Stations (PNW 95-0730).

Literature Cited

Akpo, L. E. 1993. Influence du couvert ligneux sur la structure et le fonctionnement de la strate herbacee en milieu sahelien. ORSTOM, Paris, France.

Allen, L. H., Jr., M. B. Kirkham, D. M. Olszyk, and C. E. Whitman, editors. 1997. Advances in carbon dioxide effects research. American Society for Agronomy (ASA) Special Publication Number 61.

Belsky, A. J. 1994. Influences of trees on savanna productivity: tests of shade, nutrients, and tree–grass competition. Ecology **75**:922–932.

Black, T. A., and F. M. Kelliher. 1989. Processes controlling understorey evapotranspiration. Philosophical Transactions of the Royal Society of London Series B **324**:207–231.

Black, T. A., C. S. Tan, and J. U. Nnyamah. 1980. Transpiration rate of Douglas-fir trees in thinned and unthinned stands. Canadian Journal of Soil Science **60**:625–631.

Bradshaw, L. S., J. E. Deeming, R. E. Burgan, and J. D. Cohen. 1983. The 1978 national fire danger rating system: a technical documentation. USDA Forest Service General Technical Report **INT-169,** Ogden, Utah, USA.

Canadell, J., R. B. Jackson, J. R. Ehleringer, H. A. Mooney, O. E. Sala, and E. D. Schulze. 1996. Maximum rooting depth of vegetation types at the global scale. Oecologia **108**:583–595.

Daubenmire, R. 1968. Ecology of fire in grasslands. Advances in Ecological Research **5**:201–266.

Davis, G. R., W. A. Neilson, and J. G. McDavitt. 1983. Root distribution of *Pinus radiata* related to soil characteristics in five Tasmanian soils. Australian Journal of Soil Research **21**:165–171.

Dhyani, S. K., P. Narain, and R. K. Singh. 1990. Studies on root distribution of five multi-purpose tree species in the Doon Valley, India. Agroforestry Systems **12**:149–161.

Eagleson, P. S., and R. I. Segarra. 1985. Water-limited equilibrium of savanna vegetation systems. Water Resources Research **21**:1483–1493.

Eastham, J., and C. W. Rose. 1990. Tree/pasture interactions in a range of tree densities in an agroforestry experiment. I. Rooting patterns. Australian Journal of Agricultural Research **41**:683–695.

Ehleringer, J. R., S. L. Phillips, W. S. F. Schuster, and D. R. Sandquist. 1991. Differential utilization of summer rains by desert plants. Oecologia **88**:430–434.

Ellenberg, H. 1978. Die Vegetation Mitteleuropas mit den Alpen in ökologischer Sicht. Stuttgart, Germany.

Fosberg, M. A. 1971. Moisture content calculations for the 100-hour timelag fuel in fire danger rating. USDA Forest Service Research Note **RM-199,** Fort Collins, Colorado, USA.

Fosberg, M. A., and J. E. Deeming. 1971. Derivation of the 1- and 10-hour timelag fuel moisture calculations for fire danger rating. USDA Forest Service Research Note **RM-207,** Fort Collins, Colorado, USA.

Fosberg, M. A., R. C. Rothermal, and P. A. Andrews. 1981. Moisture content calculations for 1000-hr fuels. Forest Science **27**:(1)19–26.

Gartner, F. R., and W. W. Thompson. 1972. Fire in the Black Hills forest–grass ecotone. Proceedings of the Tall Timbers Fire Ecology Conference **12**:37–68.

Gilmanov, T. G., W. J. Parton, and D. S. Ojima. 1997. Testing the CENTURY ecosystem level model on data sets from eight grassland sites in the former USSR representing a wide climatic/soil gradient. Ecological Modelling **96**:191–210.

Gupta, S. C., and W. E. Larson. 1979. Estimating soil water retention characteristics from particle size distribution, organic matter content and bulk density. Water Resources Research **15**:1633–1635.

Howard, E. A. 1978. A simple model for estimating the moisture content of living vegetation as potential wildfire fuel. Pages 20–23 *in* Fifth Conference on Fire and Forest Meteorology, 14–16 March, Atlantic City, New Jersey. American Meteorological Society, Boston, Massachusetts, USA.

Jackson, R. B., J. Canadell, J. R. Ehleringer, H. A. Mooney, O. E. Sala, and E. D. Shulze. 1996. A global analysis of root distributions for terrestrial biomes. Oecologia **108**: 389–411.

Jackson, R. B., H. A. Mooney, and E. D. Schulze. 1997. A global budget for fine root biomass, surface area and nutrient contents. Proceedings of the National Academy of Sciences (USA) **94**:7362–7366.

Jackson, R. B., H. J. Schenk, E. G. Jobbágy, J. Canadell, G. D. Colello, R. E. Dickinson, C. B. Field, P. Friedlingstein, M. Heimann, K. Hibbard, D. W. Kicklighter, A. Kleidon, R. P. Neilson, W. J. Parton, O. E. Sala, and M. T. Sykes. 2000. Belowground consequences of vegetation change and their treatment in models. Ecological Applications **10**: 470–483.

Jarvis, P. G., and J. W. Leverenz. 1983. Productivity of temperate, deciduous, and evergreen forests. Pages 234–280

in O. L. Lange, P. S. Nobel, C. B. Osmond, and H. Ziegler, editors. Encyclopedia of plant physiology. Volume 12D. Springer-Verlag, Berlin, Germany.

Jobbágy, E. G., and R. B. Jackson. 2000. The vertical distribution of soil organic carbon and its relation to climate and vegetation. Ecological Applications **10**:423–436.

Jones, T. C., R. E. Carnell, J. F. Crossley, J. M. Gregory, J. F. B. Mitchell, C. A. Senior, S. F. B. Tett, and R. A. Wood. 1997. The second Hadley Centre coupled ocean–atmosphere GCM: model description, spinup and validation. Climate Dynamics **13**:103–134.

Jonsson, K., L. Fidjeland, J. A. Meghembe, and P. Hogbert. 1988. The vertical distribution of fine roots of five tree species and maize in Morogoro, Tanzania. Agroforestry Systems **6**:63–69.

Keane, R. E., C. C. Hardy, K. C. Ryan, and M. A. Finney. 1997. Simulating effects of fire on gaseous emissions and atmospheric carbon fluxes from coniferous forest landscapes. World Resource Review **9**:177–205.

Kelliher, F. M., D. Whitehead, K. J. McAnaney, and M. J. Judd. 1990. Partitioning evapotranspiration into tree and understorey components in two young *Pinus radiata* D. Don stands. Agricultural and Forest Meteorology **50**:211–227.

Knoop, W. T., and B. H. Walker. 1985. Interactions of woody and herbaceous vegetation in a southern African savanna. Journal of Ecology **73**:235–253.

Lawson, G. W., J. Jenik, and K. O. Armstrong-Mensak. 1968. A study of a vegetation catena in Guinea savanna at Mole Game Reserve (Ghana). Journal of Ecology **56**:505–522.

Lee, C. A., and W. K. Lauenroth. 1994. Spatial distributions of grass and shrub root systems in the shortgrass steppe. American Midland Naturalist **132**:117–123.

Lenihan, J. M., C. Daly, D. Bachelet, and R. P. Neilson. 1998. Simulating broad-scale fire severity in a dynamic global vegetation model. Northwest Science **72**:(Special Issue): 91–103.

Lenihan, J. M., and R. P. Neilson. 1993. A rule-based formation model for Canada. Journal of Biogeography **20**: 615–628.

Le Roux, X., T. Bariac, and A. Mariotti. 1995. Spatial partitioning of the soil water resource between grass and shrub components in a West African savanna. Oecologia **104**: 147–155.

Lieth, H. 1975. Primary production of the major vegetation units of the world. Pages 203–205 *in* H. Lieth and R. H. Whittaker, editors. Primary productivity of the biosphere. Ecological Studies 14. Springer-Verlag, Germany.

Linacre, E. T. 1977. A simple formula for estimating evaporation rates in various climates, using temperature data alone. Agricultural Meteorology **18**:409–424.

Mack, F., J. Hoffstadt, G. Esser, and J. G. Goldammer. 1996. Modeling the influence of vegetation fires on the global carbon cycle. Pages 149–159 *in* J. S. Levine, editor. Biomass burning and climate change. MIT Press, Cambridge, Massachusetts, USA.

Matthews, E. 1983. Global vegetation and land use: new high-resolution data bases for climate studies. Journal of Climate and Applied Meteorology **22**:474–487.

Means, J. E., H. A. Hansen, G. J. Koerper, P. B. Alaback, and M. W. Klopsch. 1994. Software for computing plant biomass: BIOPAK users guide. USDA Forest Service General Technical Report **PNW-340,** Corvallis, Oregon, USA.

Menaut, J. C. 1971. Étude de quelques peuplements ligneux d'une savanne guinéenne de Côte d'Ivoire. Dissertation. Faculté des Sciences de Paris, Paris, France.

Mordelet, P., and J. C. Menaut. 1995. Influence of trees on aboveground production dynamics of grasses in a humid savanna. Journal of Vegetation Science **6**:223–228.

Mordelet, P., J. C. Menaut, and A. Mariotti. 1997. Tree and grass rooting patterns in an African humid savanna. Journal of Vegetation Science **8**:65–70.

Nambiar, E. K. S. 1990. Interplay between nutrients, water, root growth and productivity in young plantations. Forest Ecology and Management **30**:213–232.

Nambiar, E. K. S. and R. Sands. 1992. Effects of compaction and simulated root channels in the subsoil on root development, water uptake and growth of radiata pine. Tree Physiology **10**:297–306.

Neilson, R. P. 1995. A model for predicting continental-scale vegetation distribution and water balance. Ecological Applications **5**:362–385.

Neilson, R. P., J. M. Lenihan, and C. Daly. 1996. Modeling the effect of global change on grassland distribution and productivity at landscape to regional scales. Pages 73–76 *in* Toward an integrated regional research program on global change and the nation's major grasslands. 1995–1996 Annual Report of the Great Plains Regional Center. National Institute for Global Environmental Change, U.S. Department of Energy. Institute of Agriculture and Natural Resources, University of Nebraska, Lincoln, Nebraska, USA.

Okali, D. U. U., J. B. Hall, and G. W. Lawson. 1973. Root distribution under a thicket clump on the Accra plain, Ghana: its relevance to clump localization and water relations. Journal of Ecology **61**:439–454.

Parton, W. J., D. S. Schimel, C. V. Cole, and D. S. Ojima. 1987. Analysis of factors controlling soil organic matter levels in Great Plains grasslands. Soil Science Society of America Journal **51**:1173–1179.

Parton, W. J., D. S. Schimel, D. S. Ojima, and C. V. Cole. 1994. A general study model for soil organic matter dynamics, sensitivity to litter chemistry, texture, and management. Soil Science Society of America Journal. Quantitative Modeling of Soil Forming Processes, SSSA Special Publication **39**:147–167.

Peterson, D. L., and K. C. Ryan. 1986. Modeling postfire conifer mortality for long-range planning. Environmental Management **10**:797–808.

Prentice, I. C., W. Cramer, S. Harrison, R. Leemans, R. A. Monserud, and A. M. Solomon. 1992. A global biome model based on plant physiology and dominance, soil properties and climate. Journal of Biogeography **19**:117–134.

Price, D. T., T. A. Black, and F. M. Kelliher. 1986. Effects of salal understory removal on photosynthetic rate and stomatal conductance of young Douglas-fir trees. Canadian Journal of Forest Research **16**:90–97.

Probert, M. E., B. A. Keating, J. P. Thompson, and W. J. Parton. 1995. Modelling water, nitrogen, and crop yield for a long-term fallow management experiment. Australian Journal of Experimental Agriculture **35**:941–950.

Roberts, J., C. F. Pymar, J. S. Wallace, and R. M. Pitman. 1980. Seasonal changes in leaf area, stomatal and canopy conductances and transpiration from bracken below a forest canopy. Journal of Applied Ecology **17**:409–422.

Rothermel, R. E. 1972. A mathematical model for fire spread predictions in wildland fuels. USDA Forest Service Research Paper **INT-115,** Ogden, Utah, USA.

Sala, O. E., R. A. Golluscio, W. K. Lauenroth, and A. Soriano. 1989. Resource partitioning between shrubs and grasses in the Patagonian steppe. Oecologia **81**:501–505.

Sands, R., and E. K. S. Nambiar. 1984. Water relations of *Pinus radiata* in competition with weeds. Canadian Journal of Forest Research **14**:233–237.

Sarmiento, G. 1984. The ecology of neotropical savannas. Harvard University Press, Cambridge, Massa.

Scholes, R. J., and S. R. Archer. 1997. Tree–grass interactions in savannas. Annual Review Ecology and Systematics **28**: 517–544.

Scholes, R. J., and B. H. Walker. 1993. An African savanna:

Synthesis of the Nylsvley study. Cambridge University Press, Cambridge, UK.
Skarpe, C. 1992. Dynamics of savanna ecosystems. Journal of Vegetation Science **3**:293–300.
Stanek, W., and D. State. 1978. Equations predicting productivity (biomass) of trees, shrubs and lesser vegetation based on current literature. Environment Canada Forestry Service, Report **183**.
Steward, F. R., S. Peter, and J. B. Richon. 1990. A method for predicting the depth of lethal heat penetration into mineral soils exposed to fires of various intensities. Canadian Journal of Forest Research **20**:919–926.
Stone, E. L., and P. J. Kalisz. 1991. On the maximum extent of tree roots. Forest Ecology and Management **46**:59–102.
Trumbore, S. E. 2000. Age of soil organic matter and soil respiration: radiocarbon constraints on belowground C dynamics. Ecological Applications **10**:399–411.
van Wagner, C. E. 1973. Height of crown scorch in forest fires. Canadian Journal of Forest Research **3**:373–378.
van Wagner, C. E. 1993. Prediction of crown fire behavior in two stands of jack pine. Canadian Journal of Forest Research **23**:442–449.
VEMAP members. 1995. Vegetation/ecosystem modeling and analysis project: comparing biogeography and biogeochemistry models in a continental-scale study of terrestrial ecosystem responses to climate change and CO_2 doubling. Global Biogeochemical Cycles **9**:407–437.
Vogt, K. A., D. J. Vogt, P. A. Palmiotto, P. Boon, J. O'Hara, and H. Asbjornsen. 1996. Review of root dynamics in forest ecosystems grouped by climate, climatic forest type and species. Plant and Soil **187**:159–219.
Walker, B. H., and I. Noy-Meir. 1982. Aspects of stability and resilience of savanna ecosystems. Pages 556–590 *in* B. J. Huntley and B. H. Walker, editors. Ecology of tropical savannas. Springer-Verlag, Berlin, Germany.
Walter, H. 1971. Natural savannas. Ecology of tropical and sub-tropical vegetation. Oliver and Boyd, Edinburgh, UK.

APPENDIX A

A discussion of the methods for preparing MC1 input data for the Wind Cave study area is available in ESA's Electronic Data Archive: *Ecological Archives* A010-002-A1.

APPENDIX B

Listings of the life-form-varying biogeochemistry module parameters used in MC1 are available in ESA's Electronic Data Archive: *Ecological Archives* A010-002-A2.